IN VIVO HUMAN KIDNEY PH MAPPING AT 3T USING TIME-INTERLEAVED PARALLEL RF TRANSMISSION CEST

Ivan E Dimitrov[1,2], Masaya Takahashi[2], Koji Sagiyama[2], A. Dean Sherry[2,3], and Jochen Keupp[4]

[1]*Philips Medical Systems, Cleveland, OH, United States,* [2]*Advanced Imaging Research Center, University of Texas Southwestern Medical Center, Dallas, TX, United States,* [3]*Chemistry, University of Texas Dallas, Richardson, TX, United States,* [4]*Philips Research Europe, Hamburg, Germany*

INTRODUCTION

Abnormalities in pH are often associated with ailments such as tumor metastasis [1] and impaired kidney function [2]. Their diagnosis may thus dependent on the availability of convenient, non-invasive methods for assessment of parenchymal pH. A highly dependent pH process, chemical exchange can be followed via CEST-MRI (chemical exchange saturation transfer). While a wide array of endogenous molecules do exhibit CEST effects, these effects are concentration-dependent and thus may be difficult to quantify. An FDA approved CT contrast agent, Iopamidol, has been shown to have two sets of exchangeable protons that can be used to generate a concentration-independent CEST contrast [3, 4]. However, these animal experiments showed increased demands for the use of long and high-powered RF saturation. Previously, we reported the use of Iopamidol [5] for deriving ROI-based assessment of human kidney pH. Here, we report a respiratory-triggered CEST sequence with long and high-powered RF saturation that is enabled by parallel RF transmission for *in vivo* human kidney pH mapping on a clinical 3T scanner.

METHODS

All experiments were performed on a clinical 3T scanner (Achieva TX, Philips Healthcare, NL) with dual-channel parallel RF transmission and a 6-channel bi-planar torso coil for reception. Saturation pulses were applied during monitored free breathing in groups of two pulses (49 ms each), which were sent to the body-coil in a time-interleaved mode whereby the two independent RF channels operated alternately [7]. This allows higher power with 50% duty-cycle per amplifier. Compared to a previously used low-power mode that allowed for TFE acquisition only, this high-power mode allowed TSE-based acquisition. A single-slice fat-suppressed single-shot half-fourier TSE was used with FOV 300 x 350 mm, matrix 172 x 175, resolution 1.75 x 1.99 x 10 mm^3 (reconstructed 1.56 mm), SENSE 2 RL, echo-spacing 4.6 ms, TR/TE = 10 s/4.6 ms, and pixel BW 544 Hz. The scan time per frequency offset was two breathing cycles, or about 10 s. CEST saturation with a maximum number of saturation pulses was pre-defined and checked runtime to enable SAR-safe operation. In order to control respiratory artifacts and SAR, a respiratory trigger was used such that no RF saturation was applied in some of the breath cycles (see Fig 1). To determine the quiessent period after acquisition, the scanner checks on the breathing state and counts the end-expiratory events. This waiting time is filled with delay elements, the duration of which can be user-specified such that to allow for a sufficient period of no RF application. Three normal volunteers were scanned using an IRB-approved protocol for *i.v.* bolus-injection of 100 ml of Iopamidol at a rate of 2ml/s. The bolus was followed by 40 ml saline flush. Imaging started with a baseline CEST acquisition before Iopamidol injection, and continued for a period afterwards. For the CEST profile, 19 saturation frequency points in steps of 0.43 ppm around $\Delta\omega = \pm 4.64$ ppm, covering the two NH pools (4.2 ppm/5.5 ppm), and one far off-resonant (S0, $\Delta\omega$ = -160 ppm), saturation pulse-elements (2 × 49 ms, Sinc-Gauss), B1(sat-rms) = 2.3 µT and about 3.5 minutes scanning time. In addition, standard 2D B0 maps (two echoes, ΔTE = 1 ms) were recorded periodically throughout the exam. Maps of the asymmetric magnetization transfer ratio MTR(asym) = (S[-$\Delta\omega$] - S[+$\Delta\omega$]) / S0 were calculated based on ΔB0-corrected, point-by-point interpolated images S[-$\Delta\omega$] and S[+$\Delta\omega$]. For pH mapping, a ratio of the two exchangeable pools was obtained by Eq. 1 [4]. This ratio was then converted to pH values using phantom calibration curve for pH(R) that was obtained from Iopamidol phantoms at different pH values.

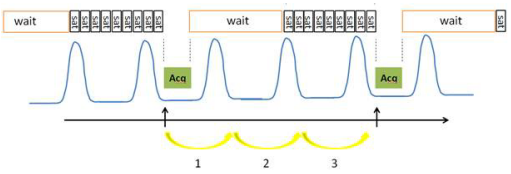

Figure 1: Improved respiratory triggered CEST. Saturation is applied continuously over multiple breathing cycles. An additional waiting time is introduced after acquisition, to allow high-power saturation, while reducing the overall SAR in a 10 s interval.

$$R = \frac{(1 - MTR_{asym}[4.2\,ppm])\,MTR_{asym}[5.5\,ppm]}{(1 - MTR_{asym}[5.5\,ppm])\,MTR_{asym}[4.2\,ppm]} \qquad [1]$$

RESULTS AND DISCUSSION

Figure 2 shows maps of the parallel transmission CEST TSE. Pre- and post-injection maps clearly show up to 20% CEST effect, especially in the kidney pelvic area. Medullar parenchymal enhancement is also seen. Both 4.2 ppm and 5.5 ppm offsets present sufficient CEST effect to allow for pixel-based pH calculation (third row). Figure 3 shows the time course of the pH in the kidney following Iopamidol injection.

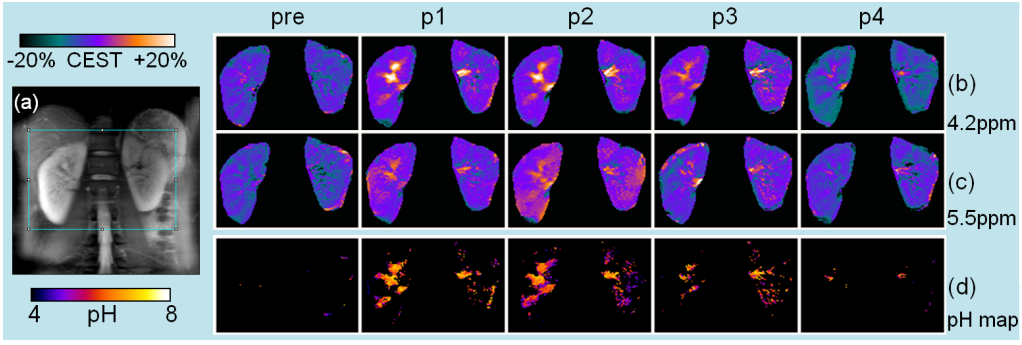

Figure 2: Respiratory-triggered Iopamidol CEST TSE imaging based on parallel RF transmission. **(a)** Selected saturation offset image (S0). Time series (pre-contrast until 20 minutes post-contrast) of the CEST effect at 4.2 ppm **(b)** and 5.5 ppm **(c)**. pH maps **(d)** as obtained via the calibrated ratiometric method (masked for voxels with significant CEST contrast >1%).

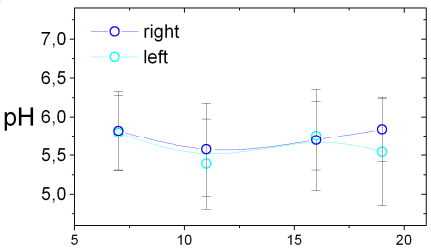

Figure 3: Analysis of the pH time course post-injection for right and left kidney (ROI covering the renal medulla and pelvis).

To the best of our knowledge, this is the first pixel-wise human pH kidney mapping using a clinically approved contrast agent. The presented technique runs in clinically relevant times and shows promising concentration-independent pH contrast that may find application in diagnosing a variety of kidney abnormalities.

ACKNOWLEDGEMENTS This work was done with the support of NIH grants CA-115531 and RR-02584.

REFERENCES [1] Gillies RJ et al., IEEE Eng Med Biol Mag 23:57 (2004) [2] Periera PC et al., Curr Genomics 10:51 (2009) [3] Aime S et al., MRM 53:830 (2005) [4] Longo DL et al., MRM 65:202 (2011) [5] Keupp J et al., Proc. ISMRM 18:828 (2010) [6] Keupp J et al., ISMRM 19:710 (2011)